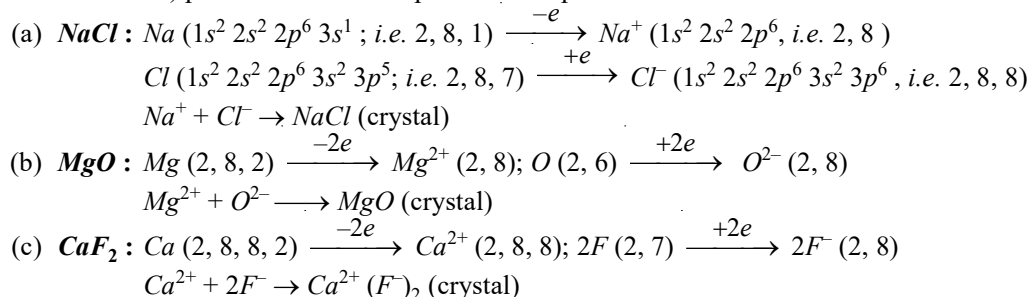# 12

Structure, Bonding and Properties of Ionic Solids and Solid State Chemistry

12.1 CHARACTERISTIC PROPERTIES OF IONIC COMPOUNDS

(i) Complete Transfer of Electron(s) from One Species to the Other

The electrovalent or ionic bond is formed between the combining species through the complete transfer of one or more valence electron(s) from one species to the other. By transferring the electron(s), the species transforms into a cation while the other species by accepting the electron(s) transforms into an anion. The electrostatic Coulombic attraction between the oppositely charged species (*i.e.* cation and anion) prevails to hold the species. Examples:

(a) **NaCl :** Na ($1s^2\,2s^2\,2p^6\,3s^1$; *i.e.* 2, 8, 1) $\xrightarrow{-e}$ Na^+ ($1s^2\,2s^2\,2p^6$, *i.e.* 2, 8)

Cl ($1s^2\,2s^2\,2p^6\,3s^2\,3p^5$; *i.e.* 2, 8, 7) $\xrightarrow{+e}$ Cl^- ($1s^2\,2s^2\,2p^6\,3s^2\,3p^6$, *i.e.* 2, 8, 8)

$Na^+ + Cl^- \rightarrow NaCl$ (crystal)

(b) **MgO :** Mg (2, 8, 2) $\xrightarrow{-2e}$ Mg^{2+} (2, 8); O (2, 6) $\xrightarrow{+2e}$ O^{2-} (2, 8)

$Mg^{2+} + O^{2-} \longrightarrow MgO$ (crystal)

(c) **CaF$_2$:** Ca (2, 8, 8, 2) $\xrightarrow{-2e}$ Ca^{2+} (2, 8, 8); $2F$ (2, 7) $\xrightarrow{+2e}$ $2F^-$ (2, 8)

$Ca^{2+} + 2F^- \rightarrow Ca^{2+} (F^-)_2$ (crystal)

(ii) Nondirectional Combining Force

The attractive force between the cationic and anionic species is purely electrostatic in nature and it is equally probable in all directions. Thus the ionic forces are quite strong and omnidirectional while the covalent forces are very much directional. The attractive Coulombic force within the ion pair is given by, $F = q^+q^-/(4\pi\varepsilon_0 r^2)$ where q^+ and q^- are the charges of the cation and anion respectively and r stands for the interionic separation. In a solid crystal, ε_0 stands for the permitivity of vacuum. The attractive force extends throughout the lattice.

(iii) Physical State

Because of the omnidirectional nature of the ionic forces, the ionic compounds form three dimensional solid aggregates of the cations and anions which are arranged in some well defined geometrical patterns. Thus the electrovalent compounds form crystalline solids. They never exist as the isolated molecules in contrast to the covalent molecules. At ordinary conditions, they remain as solids.

(iv) Electrical Conductivity

In the solid state, the ions remain in the well defined lattice points and they cannot move freely to conduct electricity. But on fusion, the ions can move freely to carry electricity. In some cases, the

conductivity of the ionic solids may rise due to the crystal defects. When the ionic compounds are dissolved in water, the ions become more free to move and as a result, the solutions are very good conductors of electricity.

(v) Hardness and Brittleness

The ionic compounds are hard because of the **omnidirectional strong electrostatic force extending throughout the crystal** but they are brittle. When an external pressure is exerted on the ionic crystal, it may set up the anion-anion and cation-cation repulsions. Because of the repulsive forces, the crystals break down. It explains the *cleavage properties of many minerals*.

(vi) Melting and Boiling Points

The reason behind the hardness can again explain the high melting and boiling points of the ionic solids.

(vii) Solubility

The ionic compounds are generally soluble in polar solvents having high dielectric constants or permitivities. It is known that the Coulombic attractive force holding the oppositely charged ions is inversely proportional to the permitivity (ε) of the medium, *i.e.* $F \propto 1/\varepsilon$. The **relative permitivities** of the different media are : air or vacuum (1), H_2O (82), CH_3CN (33), NH_3 (25). Thus with the increase of permitivity of a medium, the attractive force between the oppositely charged species decreases. This is why, when an ionic compound is placed in water, the attractive force responsible for holding the oppositely charged ions in the crystal lattice is significantly dropped to facilitate the breakage of the crystal lattice. **In general, a solvent with a higher permitivity is more promising to dissolve the ionic solids.**

The phenomenon can also be interpreted in terms of **ion-dipole interaction.** The energy required to break down the ionic lattice is largely compensated through the hydration energies of the cations and anions. The dipolar solvent molecules can solvate both the types of ions through the proper orientation of their polar ends.

(viii) Isomorphism (Greek *isos* means equal and *morphe* means form)

Many pairs of ionic compounds are known to crystallise simultaneously in the **same form** and they are referred to as isomorphous crystals (noted by E. Mitscherlich, a student of Berzelius). Such isomorphous compounds can crystallise simultaneously from a solution to form the **mixed crystals.** They can also form **overgrowth.** Some isomorphous pairs are given below :

Cu_2S, Ag_2S; $KClO_4$, $KMnO_4$; $ZnSO_4 \cdot 7H_2O$, $MgSO_4.7H_2O$; $NaNO_3$, $CaCO_3$; $KMnO_4$, $BaSO_4$; KIO_4, $CaWO_4$; $NiSO_4.7H_2O$, $NiPO_3F.7H_2O$; $K_2SO_4 \cdot Al_2(SO_4)_3 \cdot 24H_2O$, $(NH_4)_2SO_4.Al_2(SO_4)_3.24H_2O$

The basic condition for the isomorphism is the ***similarity of the internal structure of the crystals in all respects.*** It does not depend on the chemical properties and even also the total number of atoms (*e.g.* last pair in the above given examples). **The isomorphous crystals have similar unit cells with almost the same dimensions, *i.e.*, the same interfacial angle and axial ratio.** But the crystals with almost the same crystal dimensions are not necessarily isomorphous.

The detailed analysis of the isomorphous compounds reveals that for the isomorphism (characterised by the ***mixed crystal formation* and *overgrowth***), the following conditions must be satisfied.

(a) The two compounds must have the **same type of formula** to provide the **same number of lattice points** (not necessarily the same number of atoms, the atoms can be replaced by some suitable radicals to maintain the constancy of the number of lattice points).

(b) The **size** of the corresponding constituent units must be comparable.

(c) The **stereochemical orientation** of the corresponding constituent units in the compounds must be identical.

(d) The **polarising power** and **polarisability** of the corresponding constituent units in the compounds must be comparable.

(e) The crystals should have the **same type of crystal structure** (*i.e.* the same type of unit cell) with the **comparable crystal dimensions** (*i.e.* interfacial angle and axial ratio).

(f) The **molar volume** of the compounds should be comparable.

The fulfilment of the above conditions can be illustrated through the following examples.

***NaNO$_3$ and CaCO$_3$ (calcite)*:** Molar volume (in cm^3 mol^{-1}) of $NaNO_3$ = 37.4; Molar volume of $CaCO_3$ = 36.9; r_{Na^+} = 95 pm; $r_{Ca^{2+}}$ = 99 pm. Both CO_3^{2-} and NO_3^- are planar where three oxygen atoms are at the corners of an equilateral triangle. Both the central atoms (*i.e.* C and N) are sp^2 hybridised. The axial ratios of the unit cells are also comparable. Hence $NaNO_3$ and $CaCO_3$ are **isomorphous.**

***NaNO$_3$ and KNO$_3$*:** r_{Na^+} = 95 pm < r_{K^+} = 133 pm. Thus, the relative size ratio, r_+/r_- is different for $NaNO_3$ with respect to that of KNO_3. Hence these are **not isomorphous.**

***BaSO$_4$ and KMnO$_4$*:** $r_{Ba^{2+}}$ = 135 pm, r_{K^+} = 133 pm. Both MnO_4^- and SO_4^{2-} are tetrahedral and their sizes are also comparable. The axial ratios of the unit cells are also comparable. Hence, these are **isomorphous.**

***KNO$_3$ and KClO$_3$*:** ClO_3^- is pyramidal (sp^3 hybridisation of Cl) while NO_3^- is planar (sp^2 hybridisation of N). Hence, they are **not isomorphous.**

RaSO$_4$ and BaSO$_4$*:** They are isomorphous and they can be ***isomorphously coprecipitated. From the standpoint of ionic radii, Ra^{2+} (152 pm) and Ba^{2+} (143 pm) are close and they can produce **isomorphous crystals.** Ca^{2+} (106 pm) is much smaller and $CaSO_4$ is **not isomorphous** with $RaSO_4$. From a solution having a very low concentration of Ra^{2+} (*i.e.* $[Ra^{2+}][SO_4^{2-}] < K_{sp}$), it can be coprecipitated with $BaSO_4$. By using this ***carrier or collector technique,*** Ra^{2+} can be separated even when Ra^{2+} concentration in solution is exceedingly small.

Note **:** Isomorphous crystals lead to ***coprecipitation or induced precipitation*** which is important in analytical chemistry (*cf.* Sec. 14.17.3).

(ix) Variable Electrovalency

Generally the d and f block elements show variable valencies. For the d block elements (*i.e.* transition metals), the d levels remain incompletely filled for which the successive ionisation potentials do not increase too rapidly (see Sec. 8.12.2). The energy required to raise the oxidation state from a lower oxidation state can be compensated through the higher lattice energy (or, solvation energy in solution). This is why, under the identical conditions, the existence of more than one stable oxidation state becomes energetically possible. Thus the occurrence of Fe^{2+} and Fe^{3+}; Cu^+ and Cu^{2+}; Co^{2+} and Co^{3+}; etc. are well documented. **The heavier congeners (*i.e.* 4d and 5d series) show a marked tendency towards the higher oxidation state** (see Sec. 8.20.3 for ***relativistic effects***). For example, though both the +2 and +3 states are known for Co, for Rh and Ir the +3 state (or, higher state) is more well documented; stability of +4 state runs as $Pt > Pd > Ni$; Cr^{3+} is the most stable state for Cr while both Mo and W possess the stable +6 state. To explain such variable oxidation states both the *lattice energy* (*i.e. Madelung energy*) and *ligand field effects* are to be considered.

To consider the effect of ionisation potentials on the variable oxidation states, let us consider, Cu, Ag and Au which display the common states +1 and +3; but the **stability of the +3 state increases in descending the group** (*cf.* **relativistic effects,** Sec. 8.20.3). On the other hand, the stability of +2 state decreases in descending the group. The ionisation energies (kJ mol^{-1}) of Cu, Ag and Au are given in Table 12.1.1.

Table 12.1.1. Ionisation energies of *Cu*, *Ag* and *Au*

| Element | Ionisation energy ($kJ\,mol^{-1}$) | | | | |
	1st	*2nd*	*3rd*	*1st + 2nd + 3rd*	*1st + 2nd*
Cu	745	1959	3551	6255	2704
Ag	731	2074	3361	6166	2805
Au	889	1939	2943	5771	2828

Thus it is evident that to attain the trivalency (+3), the less energy is required for *Au* compared to *Cu* and *Ag* while for the +2 state, *Cu* is more favoured compared to *Ag* and *Au*. However to explain the relative stabilities of the states, consideration of the ligand field effect is extremely important. For the present system, the ***Jahn-Teller effect*** is extremely important. The ninth electron (d^9-system) in $d^1_{x^2-y^2}$ orbital (*z*-out distortion) is **destabilised maximum in *Au*(II).** It favours the oxidation of *Au*(II) to *Au*(III) compared to oxidation of *Cu*(II) and *Ag*(II).
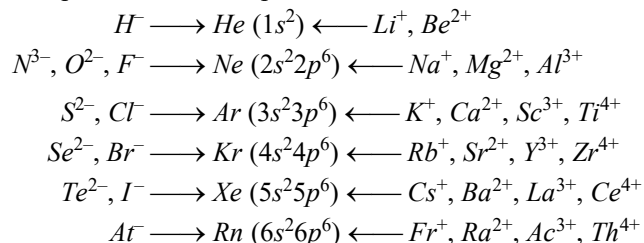
Similar arguments also hold good for the variable valencies in the lanthanides and actinides.

Lastly, the ***inert pair effect*** (see Sec. 10.3) in the just post-transition elements also leads to the variable valency.

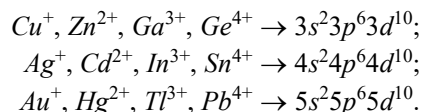## 12.2 DIFFERENT TYPES OF IONS AND ELECTRONIC CONFIGURATIONS OF THE IONS INVOLVED IN IONIC BONDING

(i) Inert Gas Structure

The ions tend to have the inert gas configuration, ns^2np^6 (exception : Be^{2+}, Li^+ and H^- of $1s^2$ helium gas structure; H^+ , no outer electron). The configuration is attained by the elements (*i.e.* metals) of Gr I (1), II (2) and III (13) by the way of complete loss of their valence electrons and by the elements (*i.e.* nonmetals) of Gr VII (17), VI (16) and V (15) by the way of capturing 1, 2 and 3 electrons respectively. Some representative examples are shown below.

$$H^- \longrightarrow He\ (1s^2) \longleftarrow Li^+,\ Be^{2+}$$
$$N^{3-},\ O^{2-},\ F^- \longrightarrow Ne\ (2s^22p^6) \longleftarrow Na^+,\ Mg^{2+},\ Al^{3+}$$
$$S^{2-},\ Cl^- \longrightarrow Ar\ (3s^23p^6) \longleftarrow K^+,\ Ca^{2+},\ Sc^{3+},\ Ti^{4+}$$
$$Se^{2-},\ Br^- \longrightarrow Kr\ (4s^24p^6) \longleftarrow Rb^+,\ Sr^{2+},\ Y^{3+},\ Zr^{4+}$$
$$Te^{2-},\ I^- \longrightarrow Xe\ (5s^25p^6) \longleftarrow Cs^+,\ Ba^{2+},\ La^{3+},\ Ce^{4+}$$
$$At^- \longrightarrow Rn\ (6s^26p^6) \longleftarrow Fr^+,\ Ra^{2+},\ Ac^{3+},\ Th^{4+}$$

(ii) The Eighteen Electron Structure (*i.e.* pseudo noble gas configuration)

The anions (**exception : Au^-** in *CsAu*, $Au^- \rightarrow 5s^25p^65d^{10}$) do not have the 18 electron structure, but it is frequently observed for the cations of the post-transition elements. The post-transition elements of Gr I (11), II (12), III (13) and IV (14) lose their outermost electrons $1(ns^1)$, $2(ns^2)$, $3(ns^2np^1)$ and $4(ns^2np^2)$ respectively to attain the electronic structure, $(n-1)s^2(n-1)p^6(n-1)d^{10}$. Some examples are:

$$Cu^+,\ Zn^{2+},\ Ga^{3+},\ Ge^{4+} \rightarrow 3s^23p^63d^{10};$$
$$Ag^+,\ Cd^{2+},\ In^{3+},\ Sn^{4+} \rightarrow 4s^24p^64d^{10};$$
$$Au^+,\ Hg^{2+},\ Tl^{3+},\ Pb^{4+} \rightarrow 5s^25p^65d^{10}.$$

In this category *Cu*, *Ag* and *Au* show the variable oxidation states of +1, +2, +3 characterised by 18, 17 and 16 outermost electrons respectively. The general stability orders are [see Sec. 12.1 (ix)] :
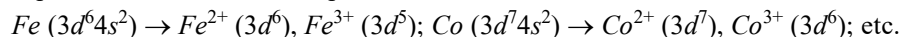
$$Cu^{2+} > Cu^+ \gg Cu^{3+};\ Ag^+ > Ag^{2+};\ Au^{3+} > Au^+ \gg Au^{2+}.$$
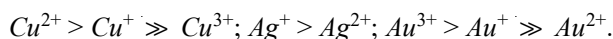
It shows that the attainment of just outermost 18 electron structure cannot assure the stability necessarily. It is proposed by some authors that the nuclear charges of these species are not sufficiently high to bind the outermost 18 electrons firmly. It is highly pronounced (see Table 12.1.1) in the case of Au which leads to +3 state as the most stable one. But Zn^{2+}, Cd^{2+}, Hg^{2+}, etc. attain the stability with the 18 electron structure. Thus the explanation is not correct. *The relative stability of such variable oxidation states can be rationalised by the simultaneous consideration of the* ***endothermic effect*** *(i.e. ionisation energy) and the* ***exothermic effects*** *(i.e. lattice or solvation energy and ligand field stabilisation energy).*

For the heavier post-transition elements, due to the ***inert pair effect*** (see Sec. 10.3), instead of the 18 electron structure, the **18, 2 structure**, *i.e.* $(n-1)s^2(n-1)p^6(n-1)d^{10}ns^2$, is preferred. Some representative examples are : Tl^+, Pb^{2+}, $Bi^{3+} \rightarrow 2, 8, 18, 32, 18, 2$; $Sb^{3+} \rightarrow 2, 8, 18, 18, 2$.

(iii) The Transition and Inner-transition Metal Ion Structure

The transition metal ions are characterised by $(n-1)s^2(n-1)p^6(n-1)d^{1-9}$. The incompletely filled d-level shows the variable valency because of the small difference in stability of two or more oxidation states for a particular metal. For example :

$$Fe\ (3d^6 4s^2) \rightarrow Fe^{2+}\ (3d^6),\ Fe^{3+}\ (3d^5);\ Co\ (3d^7 4s^2) \rightarrow Co^{2+}\ (3d^7),\ Co^{3+}\ (3d^6);\ \text{etc.}$$

For the inner-transition metal ions (*i.e.* lanthanides and actinides), the incompletely $(n-2)f$ filled level leads to the variable valency. The electronic configuration of the inner-transition metal ions is given by $(n-2)d^{10}(n-2)f^{1-13}(n-1)s^2(n-1)p^6$, ($n = 6$ for lanthanides, $n = 7$ for actinides).

(iv) Polyatomic Ions

Many covalently bonded polyatomic species can act as the constituent ions in some ionic crystals. Such anions are: CO_3^{2-}, NO_3^-, BF_4^-, BeF_4^{2-}, MnO_4^-, ClO_4^-, CrO_4^{2-}, SO_4^{2-}, $[Fe(CN)_6]^{3-/4-}$, etc. and such cations are: NH_4^+, $[Cu(NH_3)_4]^{2+}$, $[Co(NH_3)_6]^{3+}$, etc.

(v) Ions with Irregular Configurations

There are some polynuclear cluster species which cannot be classified into any particular group. Examples: Hg_2^{2+}, Ge_2^{2+}, etc.

12.3 ELECTRON DENSITY (ED) MAPS AND IONIC RADII

12.3.1 Ionic Radii from X-Ray Electron Density Maps

The X-ray studies can precisely determine the internuclear distance, but it cannot estimate directly the size of the individual ions which is governed by the radial distribution probability of the outermost electrons. But it can record the electron density maps (ED maps) which arise due to the scattering of the X-rays by the electrons. From the ED maps, it is observed that the electron density gradually falls from the nucleus of an ion with the increase of the distance along the internuclear axis of the adjacent ions and at a particular distance it falls to a minimum value then it rises gradually as the distance towards the nearest next nucleus decreases (see Fig. 12.3.1.1). ***Now we can assume that at the point of minimum electron density, one ion stops and the next one starts.*** Thus we may define an ionic radius of an ion as the distance from its nucleus to the point of
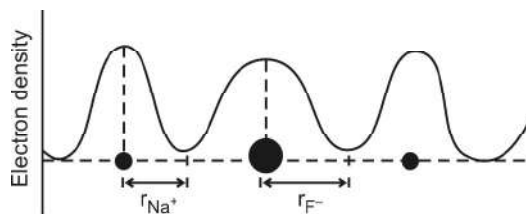

Fig. 12.3.1.1. Electron density (ED) maps in NaF crystals (variation of electron density around the nuclei).

minimum electron density along the line joining the centres of the adjacent two ions (*i.e.* generally cation and anion). Some representative values of ionic radii obtained from X-ray electron density maps of alkali halides are given in Table 12.3.1.1. Here it is worth mentioning that the ED map very often passes through a very broad minimum instead of a sharp minimum and it complicates to parametrize the size of ions.

Table 12.3.1.1. Some representative ionic radii derived from X-ray electron density maps

Ion	Ionic radius r_+ (pm)	Ion	Ionic radius r_- (pm)
Na^+	117	Cl^-	164
K^+	149	Br^-	180
Rb^+	163	I^-	205
Cs^+	186		

In comparison with the ionic radii obtained from other methods (say, Pauling's method, see Table 12.3.2.1), these values are different.

12.3.2 Ionic Radii from Other Methods

In the crystals, the ions are at an equilibrium distance where the attractive and repulsive forces balance each other. This equilibrium internuclear distance can be easily obtained from the *X*-ray studies. The internuclear separation (R_0) is the sum of the radii of the involved ions, *i.e.* $R_0 = r_+ + r_-$. Thus if the radius of one ion is known, then by subtraction, the radius of the other ion can be obtained. To solve the problem, ***it is assumed that the ionic radius of an ion is its own characteristic property and it is constant and it does not depend on the neighbour with which it exists.*** This approximation is at least grossly supported from the experimental fact. For example, the difference between the radii of K^+ and Na^+ ions derived from the measurements of four different alkali halides is fairly constant.

$$r_{K^+} - r_{Na^+} = R_{0(KF)} - R_{0(NaF)} = 35 \text{ pm}; R_{0(KCl)} - R_{0(NaCl)} = 35 \text{ pm};$$
$$R_{0(KBr)} - R_{0(NaBr)} = 32 \text{ pm}; R_{0(KI)} - R_{0(NaI)} = 30 \text{ pm}.$$

Now to start the process to compute the ionic radii, *it is required to have the knowledge of the value of ionic radius of at least one*. Then we can go for the others by using this value. Hence, it is important to determine the ionic radius of the starting one by an independent method. The validity or accuracy of the computation process for the other ions depends on the accuracy of the starting value determined separately. Some methods developed by different workers are discussed below.

 (i) ***Lande's Method :*** Lande′ (1920) started with the crystal of *LiI* in which the size of the anion is much larger compared to that of the tiny cation, Li^+. Here it is assumed that the large sized anions touch with one another. Thus half of the internuclear separation between the adjacent anions gives the value of ionic radius of the anion, *i.e.* $r_{I^-} = \frac{1}{2} R_{0(I-I)} = \frac{1}{2}(426) \text{ pm} = 213 \text{ pm}$.

By using this value for I^-, the ionic radius of K^+ is evaluated as,

$$r_{K^+} = R_{0(K^+ - I^-)} - r_{I^-} = (353 - 213) \text{ pm} = 140 \text{ pm}.$$

By continuing the process, ionic radii for the other ions have been determined.

(ii) ***Bragg's Method :*** Bragg in 1927 assumed the radius of O^{2-} as half of the internuclear distance of the adjacent oxide ions in silicates. Thus Bragg started with the silicate in the same way as followed by Lande′ in the case of *LiI*. Thus, $r_{O^{2-}} = \frac{1}{2} R_{0(O-O)}$ in silicate, $= \frac{1}{2}(270) \text{ pm} = 135$ pm. By using this value, Bragg and West computed the ionic radii for more than 80 ions.

(iii) *Molar Refractivity Method* : *Goldschmidt's Radii* : By using the Lorentz-Lorenz equation (see Eq. 12.3.2.1), the molar refraction (R_M) can be determined experimentally.

$$R_M = \frac{n^2 - 1}{n^2 + 2} \cdot \frac{M}{\rho} \qquad \qquad \text{...(12.3.2.1)}$$

where n is the refractive index of the substance of molecular mass M and density ρ. R_M is an *additive property* of the constituent atoms or ions and bonds. Thus, for the ionic compounds, the refraction by the constituent individual ions can be determined.

The molar refraction has the dimension of volume ($= M/\rho$). Thus if $R_{M(i)}$ is the ionic refraction by the i-th ion, then the radius (r_i) of the ion can be calculated as follows :

$$r_i = C R_{M(i)}^{1/3} \qquad \qquad \text{...(12.3.2.2)}$$

where C is the proportionality constant. By using the above relation, for two different ions, we have:

$$r_i/r_j = \left[\frac{R_{M(i)}}{R_{M(j)}}\right]^{1/3} \quad \text{or,} \quad \frac{r_i}{r_i + r_j} = \frac{R_{M(i)}^{1/3}}{R_{M(i)}^{1/3} + R_{M(j)}^{1/3}} \qquad \qquad \text{...(12.3.2.3)}$$

Thus if the ionic refractions of the individual ions and the corresponding interionic seperations are known, then by using Eqn. 12.3.2.3, the ionic radii of the constituent ions can be evaluated. This method was developed by Wasastjerna in 1923.

By using the interionic distances in the alkali halides and alkaline earth oxides, the ionic radii for F^- and O^{2-} are found to be 133 pm and 132 pm respectively. Goldschmidt (1929) utilised these values to compute the ionic radii for a number of ions. These values are very often referred to as *Goldschmidt's ionic radii.*

(iv) *Pauling's Method and Pauling's Univalent Radii* : Now we can recall the quantum mechanical analysis of the **hydrogen like system** for which the radius of the species having the electron in the outermost principal quantum number n is given by :

$$r_n = n^2 h^2/(4\pi m e^2 Z), \text{ in CGS unit;} \quad r_n = \varepsilon_0 n^2 h^2/(\pi m e^2 Z), \text{ in SI unit;}$$

i.e. $\qquad r_n = C n^2/Z \qquad \qquad \text{... (12.3.2.4)}$

where, C is constant, m = mass of an electron, e = charge of an electron, Ze = nuclear charge. For a many-electron species, the radial distribution function of the outermost electron determines the size of the ion and such electrons are attracted towards the nucleus. In a **polyelectronic system**, because of the screening effect, the outermost electron experiences the nuclear charge $(Z - S)e$, where S is the screening constant, which can be evaluated by the *Slater's rule* (see Sec. 4.2.4). Thus the radius of an ion can be expressed as :

$$r_{\text{ion}} = \frac{C n^2}{Z - S} = \frac{C n^2}{Z^*} \qquad \qquad \text{...(12.3.2.5)}$$

For the *isoelectronic species*, n (the outermost principal quantum number) is identical. In each of the compounds, Na^+F^-, K^+Cl^-, Rb^+Br^- and Cs^+I^-, the **constituent ion pairs are isoelectronic.** For such isoelectronic ion pairs we can write :

$$\frac{r_+}{r_-} = \frac{Z_{\text{anion}} - S}{Z_{\text{cation}} - S} = \frac{Z_{\text{anion}}^*}{Z_{\text{cation}}^*} \qquad \qquad \text{...(12.3.2.6)}$$

$C n^2$ and S are identical for the isoelectronic species, because these depend only on the electronic configuration. The constant $C n^2$ is different for different inert gas configurations. For the ions

of neon gas configuration (*e.g.* O^{2-}, F^-, Na^+, Mg^{2+}, Al^{3+}, etc.), its value is 614 pm. The value of Cn^2 for the argon gas configuration (*e.g.* K^+, Cl^-, Ca^{2+}, S^{2-}, etc.) is 1036.5 pm. Similarly it can be calculated for other species also. Eqn. 12.3.2.6 reduces to,

$$\frac{r_{cation}}{r_{cation} + r_{anion}} = \frac{Z_{anion} - S}{Z_{cation} + Z_{anion} - 2S} = \frac{Z^*_{anion}}{Z^*_{cation} + Z^*_{anion}} \qquad \ldots(12.3.2.7)$$

i.e.

$$\boxed{\frac{r_+}{r_+ + r_-} = \frac{Z^*_-}{Z^*_+ + Z^*_-}}$$

The internuclear distance ($R_0 = r_{cation} + r_{anion}$) can be obtained from the X-ray studies and the shielding constant S can be obtained by using the Slater's rule for the lighter elements, and from the values of molar refraction for the heavier members. Thus, r_+ and r_- can be easily computed.

Let us illustrate the process for Na^+F^- in which the **isosteric species are having the electronic configuration,** $1s^2 2s^2 2p^6$. The shielding constant S, for this configuration is obtained by the Slater's rule :

$$S = 7 \times 0.35 + 2 \times 0.85 = 4.15$$

The interionic separation is 231 pm, *i.e.* $r_{Na^+} + r_{F^-} = 231$ pm. Now by using Eqn. 12.3.2.7, we get:

$$\frac{r_{Na^+}}{r_{Na^+} + r_{F^-}} = \frac{Z_{F^-} - 4.15}{Z_{Na^+} + Z_{F^-} - 2 \times 4.15} = \frac{9 - 4.15}{11 + 9 - 8.30} = \frac{4.85}{11.70}$$

or,

$$r_{Na^+} = 95.7 \text{ pm and } r_{F^-} = 135.3$$

Note on calculation of Z^* : In calculating S for the **isosteric species** Na^+ and F^-, some authors consider all 8 electrons in the valence shell instead of 7 electrons shielding the last valence shell electron. It leads to :

$$S = 8 \times 0.35 + 2 \times 0.85 = 4.50, \text{ and } Z^* = 6.5 \text{ (for } Na^+\text{), and } Z^* = 4.5 \text{ (for } F^-\text{).}$$

Thus the Z^* values obtained are very close to those of Pauling's values (*cf.* 6.48 and 4.48 for Na^+ and F^- respectively). This is the justification for considering all the 8-valence electrons, but it definitely does not obey the Slater's rule. However, in this method, the calculated values: $r_+ = 94.5$ pm and $r_- = 136.5$ pm do not differ significantly from the values obtained by using the Slater's rule strictly.

In the case of K^+Cl^-, the ions are isosteric having the electronic configuration $1s^2 2s^2 2p^6 3s^2 3p^6$. The shielding constant for these isosteric ions is obtained as follows :

$$S = 7 \times 0.35 + 8 \times 0.85 + 2 \times 1.0 = 2.45 + 6.80 + 2 = 12.25$$

By using the value, $r_{K^+} + r_{Cl^-} = 314$ pm, we get :

$$\frac{r_{K^+}}{r_{K^+} + r_{Cl^-}} = \frac{Z_{Cl^-} - 11.25}{Z_{K^+} + Z_{Cl^-} - 2 \times 11.25} = \frac{17 - 11.25}{19 + 17 - 22.5} = \frac{5.75}{13.5}$$

or, $r_{K^+} = 133$ pm and $r_{Cl^-} = 181$ pm.

(v) **Pauling's Crystal Radii :** Now let us try to apply the method utilised in computing the ionic radii of **1-1 salt** (where $|Z^+| = |Z^-| = 1$) in the cases where the cationic and anionic charges are not unity. Let us take the case of CaS which has the $NaCl$ structure. The electronic configurations

of Ca^{2+} and S^{2-} are : $1s^2 2s^2 2p^6 3s^2 3p^6$ (*i.e. Ar* configuration). Thus, the ions are also isoelectronic with K^+ and Cl^-. Hence we can write :

$$r_{Ca^{2+}}/r_{K^+} = (Z_{K^+} - S)/(Z_{Ca^{2+}} - S) = \frac{19 - 11.25}{20 - 11.25}$$

Using the value of r_{K^+} obtained from *KCl*, we get, $r_{Ca^{2+}} = 117$ pm.

Similarly, by using the relation, $r_{S^{2-}}/r_{K^+} = (Z_{K^+} - 12.25)/(Z_{S^{2-}} - 12.25)$, we get, $r_{S^{2-}} = 219$ pm. These values can also be evaluated by using the constant Cn^2 (see Eqn. 12.3.2.5) which is 1036.5 pm for the argon gas configuration.

Thus we get the calculated internuclear distance, $r_{Ca^{2+}} + r_{S^{2-}} = (117 + 219)$ pm $= 336$ pm. This value is much larger than the experimentally observed value 284 pm. **Thus the process is erratic for the polyvalent ions while it is good for the *uni-univalent systems*.** In fact, radii calculated for the polyvalent ions in this way are referred to as their ***hypothetical univalent radii*** when the ions act hypothetically as the univalent ions in the Coulombic field.

To clarify the above drawback, we are to consider the **Born-Lande equation** (see Sec. 12.7.1) in which it is found that the equilibrium internuclear distance (R_0) is related as follows.

$$R_0 = \left(\frac{nB4\pi\varepsilon_0}{AZ^+ Z^- e^2} \right)^{1/(n-1)} \qquad \qquad ...(12.3.2.8)$$

It shows that the internuclear equilibrium distance (R_0) is proportional to $(1/Z^+ Z^-)^{1/(n-1)}$ for which the **Born exponent** (n) is the same for the isosteric species, *i.e.*

$$R_0 \propto (1/Z^+ Z^-)^{1/(n-1)} \qquad \qquad ...(12.3.2.9)$$

Thus if for the uni-univalent salt, the interionic separation is $R_{0(11)}$ and $R_{0(ij)}$ is the separation for the $i-j$ type lattice (*i.e.* $|Z^+| = i$, $|Z^-| = j$), then they are related as :

$$R_{0(11)} = D \left(\frac{1}{1 \times 1} \right)^{1/(n-1)} \qquad \qquad ...(12.3.2.10)$$

$$R_{0(ij)} = D \left(\frac{1}{ij} \right)^{1/(n-1)} \qquad \qquad ...(12.3.2.11)$$

where, $\qquad\qquad D = \left(\frac{nB4\pi\varepsilon_0}{Ae^2} \right)^{1/(n-1)}$

If, n and B are the same then we can write :

$$\boxed{\frac{R_{0(ij)}}{R_{0(11)}} = (1/ij)^{1/(n-1)}} \qquad \qquad ...(12.3.2.12)$$

Thus by using Eqn. 12.3.2.10, for $i - j$ type lattice, we get the ***univalent ionic radii for the multivalent ions. These are the hypothetical radii for the multivalent ions, when they retain the electronic configurations but act in the Coulombic field as the univalent ions.*** Thus Eqn. 12.3.2.10 leads to the real values only for the 1–1 type lattice structures. However, by using Eqns. 12.3.2.11–12, we can calculate the real ionic radii for the polyvalent ions by using their hypothetical univalent radii obtained from Eqn. 12.3.2.10.

For example, the isosteric species K^+, Cl^-, Ca^{2+} and S^{2-} are having the argon configuration for which the Born exponent is : $n = 9$. The internuclear distance of the hypothetical uni-univalent *CaS* is 336 pm, *i.e.* $R_{0(11)} = 336$ pm. Therefore, $R_{0(Ca^{2+}-S^{2-})} = 336 \ (1/4)^{1/(9-1)} = 336 \times 0.84 = 282.2$ pm. This calculated value is in good agreement with the observed one, 284 pm.

For calculating the ionic radii of the polyvalent ions, we can proceed as follows :

$$R_{0(ij)} = R_{0(11)} \times (ij)^{-1/(n-1)} \qquad \qquad \ldots(12.3.2.13)$$

From Eqn. 12.3.2.13, taking $i = j$, i.e. $R_{0(ij)} = 2r_i$ and $R_{0(11)} = 2r_1$, we get :

$$r_i = r_1(i)^{-2/(n-1)} \qquad \qquad \ldots(12.3.2.14)$$

where r_i = crystal field radius for the i-valent ion, and r_1 = univalent radius of the i-valent ion. Let us apply Eqn. 12.3.2.14 for Ca^{2+} and S^{2-} for which $n = 9$, $r_{1(Ca^{2+})}$ = univalent radius of Ca^{2+} = 117 pm, and $r_{1(S^{2-})}$ = 219 pm

Therefore, $r_{2(Ca^{2+})}$ = ionic radius of divalent Ca^{2+} = $117 \times (2)^{-2/8} = 117 \times 0.84 = 98.3$ pm; and, $r_{2(S^{2-})} = 219 \times 0.84 = 184$ pm.

The best value obtained in this method for the radius of O^{2-} ion is 140 pm. Using this value, Pauling estimated the ionic radii for most of the common ions. These are very often referred to as **Pauling's ionic radii.** These are given in Table 12.3.2.1 for some representative ions.

Table 12.3.2.1. Pauling's ionic radii (values in pm) for some representative ions (6:6 coordination system, $r_+/r_- = 0.7$)

Ions of main group elements

Li^+	60	Be^{2+}	31							H^-	208
Na^+	95	Mg^{2+}	65	Al^{3+} 50	Si^{4+}	41		O^{2-}	140	F^-	136
K^+	133	Ca^{2+}	99	Ga^{3+} 62	Ge^{4+}	53		S^{2-}	184	Cl^-	181
Rb^+	148	Sr^{2+}	113	In^{3+} 81	Sn^{4+}	71	Tl^+ 144	Se^{2-}	198	Br^-	195
Cs^+	169	Ba^{2+}	135	Tl^{3+} 95	Pb^{4+}	84	Pb^{2+} 120	Te^{2-}	221	I^-	216

Transition metal ions*

Ti^{4+}	68	Ti^{3+}	76	Mn^{2+}	80	Cu^+	96	Zn^{2+}	74
Zr^{4+}	80	Fe^{3+}	53	Fe^{2+}	75	Ag^+	126	Cd^{2+}	97
Ce^{4+}	101	Cr^{3+}	55	Co^{2+}	72	Au^+	137	Hg^{2+}	110
		Co^{3+}	63	Ni^{2+}	69				

* value largely depends on the spin state, *i.e.* high spin or low spin state.

(vi) *Yatsimirskii's Thermochemical Radii* **:** The methods already discussed are not suitable for the polyvalent ions such as CN^-, CO_3^{2-}, SO_4^{2-}, BF_4^-, etc. **The problem is further complicated in these cases because most of the polyvalent ions are nonspherical in shape.** But it is very often required to know their ionic radii for calculating the lattice energy of the systems involving such polyvalent ions.

To solve the problem, Yatsimirskii developed a method to calculate the ionic radii for such species from the lattice energy of the compounds containing the species by using the standard equations such as **Born-Lande equation** (see Eqns. 12.7.1.13-15), **Kapustinskii equation** (see Eqn. 12.7.4.1), etc. From such equations the interionic separation is obtained. Then if the radius of one of the ions is known, the radius for the other ion can be obtained. For example, in the case of KNO_3, the radius of K^+ is known and hence from the knowledge of interionic separation, the radius of NO_3^- can be estimated. Some representative values are given in Table 12.3.2.2.

Except for the perfectly tetrahedral ions (*e.g.* SO_4^{2-}, MnO_4^-, CrO_4^{2-}, BeF_4^{2-}, BF_4^-, ClO_4^-, etc.) and octahedral ions (*e.g.* SiF_6^{2-}, AlF_6^{3-}, PF_6^-, etc.) which tend to adopt the *spherical* **(at least pseudo-spherical) symmetry,** the thermochemical radii are of no use. However, these values can be used approximately in the thermochemical treatments.

Table 12.3.2.2. Yatsimirskii's thermochemical radii adjusted to be compatible with Shannon's crystal radii for some representative polyvalent ions.

Ion	Thermochemical radius (pm)	Ion	Thermochemical radius (pm)
NH_4^+	151	OH^-	119
$CH_3CO_2^-$	148	CN^-	177
BF_4^-	218	NO_3^-	165
CO_3^{2-}	164	NO_2^-	178
CrO_4^{2-}	242	ClO_4^-	226
MnO_4^-	215	ClO_3^-	157
SO_4^{2-}	244	BrO_3^-	140
N_3^-	181	IO_3^-	108

12.3.3 Shannon's Crystal Radii

Shannon has considered all the factors such as oxidation state, crystal structure, covalent-ionic interaction, coordination number (C.N.), crystal vacancies and distortions, etc. which influence the ionic radii. He has defined a set of crystal radii for different coordination numbers based on $r_{O^{2-}} =$ 124 pm (C.N. = 4), 126 pm (C.N. 6), = 128 pm (C.N. = 8).

12.3.4 Comparison among Shannon's Crystal radii, Goldschmidt's Radii and Pauling's Radii

The basic principles of these methods have been already discussed. Goldschmidt started with the ionic radius of O^{2-} as 132 pm while Pauling started with the value 140 pm for O^{2-}. Except for H^-, the differences in the values are not remarkable (see Table 12.3.4.1).

Table 12.3.4.1. Comparison among different types of ionic radii

Ion	Shannon's crystal radii	Goldschmidt's value (pm)	Pauling's value (pm)	Ion	Shannon's crystal radii (pm)	Goldschmidt's value (pm)	Pauling's value (pm)
H^-		154	208	Be^{2+}	59	34	31
F^-	119	133	136	Mg^{2+}	86	78	65
Cl^-	167	181	181	Ca^{2+}	126	106	99
Br^-	182	196	195	Sr^{2+}	132	127	113
I^-	206	220	216	Ba^{2+}	149	143	135
O^{2-}	126	132	140	Al^{3+}	68	57	50
S^{2-}	170	174	184	Sc^{3+}	89	83	81
Li^+	90	68	60	Y^{3+}	104	106	93
Na^+	116	98	95	Si^{4+}	54	39	41
K^+	152	133	133	Ti^{4+}	75	64	68
Rb^+	166	149	148	Zr^{4+}	86	87	80
Cs^+	181	165	169	Ce^{4+}	101	102	101

The ionic radius for H^- is astonishingly high. This high value appears due to the presence of a single charge in the nucleus which weakly binds the two outer electrons. Besides this, the electrons repel strongly each other and screen each other from facing the nuclear charge.

It is interesting to note that in the alkali hydrides, the Pauling's high value for H^- is never attained (see Table 12.3.4.2) and it gradually increases with the increase of electropositive character of the

alkali metal. *In other words, with the increase of covalency (i.e. the increase of anion polarisation by the cation), the ionic radius for H⁻ decreases.* The value reported by Goldschmidt is the crystalographic value obtained for *CsH*.

Table 12.3.4.2. Apparent radius of H^- in alkali metal hydrides.

Compound	$R_{0(M+ - H^-)}$ (pm)	$r_{H^-} = R_0 - r_{M+}$ (pm)
LiH	204	126
NaH	244	146
KH	285	152
RbH	302	153
CsH	319	154

The *nonattainability of the high value for H⁻* calculated by Pauling is due to the ***easy compressibility*** of the diffuse *H⁻* in which the electrons are loosely bound and a ***certain degree of covalency*** **(which cannot be avoided for such a polarisable anion) in the *M—H* bond. With the increase of covalency, the radius of an anion decreases.** The effect of covalency on the radius of *H⁻* is nicely reflected (see Table 12.3.4.2) in the alkali metal hydrides. In *LiH*, the covalency is maximum and hence the ionic radius of *H⁻* is minimum in *LiH*.

Compared to the *traditional ionic radii*, the *Shannon's crystal radii* are better to represent the reality. The Shannon's crystal radii take care of partial covalency present in the systems and these ionic radii are generally larger for the cations and smaller for the anions than the traditional ionic radii.

12.4 FACTORS AFFECTING THE IONIC RADII

(i) ***Principal quantum number for the outermost electrons*** **:** In general, we have the relation (see Eqn. 12.3.2.4),

$$r_{ion} = Cn^2/(Z_{ion} - S) = Cn^2/Z_{ion}^*,$$

where *C* is a constant and *n* is the principal quantum number for the outermost electrons. Thus with the increase of *n*, the radius increases. But we should simultaneously consider both the factors *n* and Z^*. If Z^* remains more or less constant then the radius increases with the *n* as in the alkali metal ions and nonmetals (specially away from the transition metals) of Gr VI (16), VII (17). But if both *n* and Z^* increase simultaneously as in the heavier transition metals, then the variation of r_{ion} with the *n* is not so marked. These aspects have been discussed in detail in discussing the ***periodic trends of radii of the ions*** (see Sec. 8.10).

Li^+ (90 pm) $< Na^+$ (116 pm) $< K^+$ (152 pm) $< Rb^+$ (166 pm) $< Cs^+$ (181 pm) **(Shannon's values)**

F^- (119 pm) $< Cl^-$ (167 pm) $< Br^-$ (182 pm) $< I^-$ (206 pm) (Shannon's values)
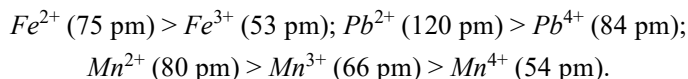

Hydrated ions vs. Bare ions

The smaller bare ions are more hydrated (*i.e.* larger hydration sphere, see Chapter 11, Vol. 2) because of their higher electrical field intensity compared to the larger bare ions. *Thus size sequence of the hydrated ions very often opposes the size sequence of the bare ions.*

Size of hydrated ions **:** $Li^+ > Na^+ > K^+ > Rb^+$

*Size of bare ions* **:** $Li^+ < Na^+ < K^+ < Rb^+$

(ii) ***Charge on the ion and nuclear charge to number of electron ratio*** **:** With the increase of positive charge (more correctly, the effective nuclear charge, Z^*) on the cation (retaining the

same principal quantum number for the outermost electrons whose radial distribution function governs the size of the ion), the outermost electrons experience an increased attraction towards the nucleus. **Thus with the increase of positive charge of the cation, there is a shrinkage in the size due to the increase of the nuclear charge/electron ratio.**

$$Fe^{2+} \text{ (75 pm)} > Fe^{3+} \text{ (53 pm)}; Pb^{2+} \text{ (120 pm)} > Pb^{4+} \text{ (84 pm)};$$

$$Mn^{2+} \text{ (80 pm)} > Mn^{3+} \text{ (66 pm)} > Mn^{4+} \text{ (54 pm)}.$$

These are the Pauling radii.

- *Corresponding covalent radii vs. ionic radii* : *The covalent or atomic radii are always larger than the cationic radii.* For examples (Pauling's value) :

    Li (152 pm) > Li^+ (60 pm) ; K (231 pm) > K^+ (133 pm); Ba (217 pm) > Ba^{2+} (135 pm).
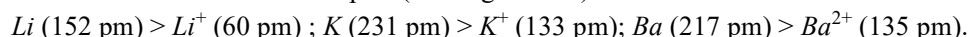
    It occurs so, because in these cations, the **outermost principal quantum number decreases** by unity compared to the neutral species. Besides this, the enhanced positive charge on the cationic species also favours the size shrinkage.

    For the anions, an increased negative charge increases the **electron-electron repulsion** and decreases the effective nuclear charge experienced by the outermost electrons and as a result, with the increase of charge on an anion, the size increases due to decrease of nuclear charge/electron ratio. *This is why, the anionic radii are larger than their corresponding covalent or atomic radii.* For examples (Pauling's value) :

    Cl^- (181 pm) > Cl (99 pm); O^{2-} (140 pm) > O (66 pm); S^{2-} (184 pm) > S (104 pm).
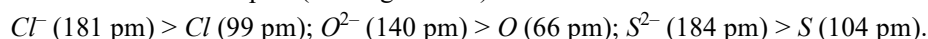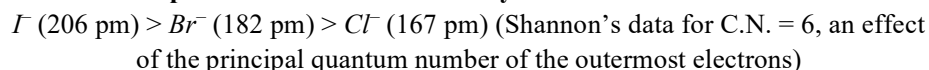
    Here it is worth mentioning that the increase of anionic charge **contracts the interionic cation-anion separation** due to the **increased Coulombic interaction.** *This fact tends to introduce a shrinkage in the anionic radius with the increase of the anionic charge.* This aspect will be illustrated in the case of *isosteric anions* (see Table 12.4.2).

- *Lanthanides and actinides* : By considering the effect of Z^* and relativistic effect, the *lanthanide and actinide contractions* have been explained in Sec. 8.9.

    La^{3+} (117 pm) > Nd^{3+} (112 pm) > Gd^{3+} (108 pm) > Ho^{3+} (104 pm) > Lu^{3+} (100 pm)
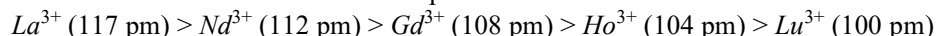
    $\longrightarrow$ Increasing trend of Z^* along the period from left to right

- *Halide vs. halate* : In this connection, it is interesting to consider the **trend of ionic radii of the halides in comparison with that of their oxyanions.**

    I^- (206 pm) > Br^- (182 pm) > Cl^- (167 pm) (Shannon's data for C.N. = 6, an effect of the principal quantum number of the outermost electrons)

    while, ClO_3^- (157 pm) > BrO_3^- (140 pm) > IO_3^- (108 pm) (thermochemical data).

    It is not fully justified to compare the thermochemical radii of the halate ions with the ionic radii of their corresponding halides, but still, *the reverse trend for the two series is really interesting*. In the halates, the central atom is in +5 oxidation state. **For the heavier congeners of X^{5+}, presence of low shielding d- and f-electrons leads to more effective nuclear charge experienced by the electrons at the periphery.**

- *Isosteric species* : Now let us consider the effect of charge on the ionic radii among the *isosteric species* having identical extranuclear configurations. **Two factors** work. (a) For the cationic isosteric species, the ionic radius decreases rapidly with the increase of positive charge due to increase of nuclear charge/electron ratio (Table 12.4.1). This is in conformity with the prediction from the relation, $r_{ion} = Cn^2/(Z_{ion} - S)$ (for the isosteric species Cn^2 is constant). (b) In addition to the above factor, the increased cationic charge attracts the coordinating surrounding anions more closely resulting a **shrinkage in the interionic separation** and hence in the ionic radii. *Thus the two factors work in the same direction to decrease the ionic radius.*

Table 12.4.1. Ionic radii of some **isosteric cations**

Ion :	Na^+	Mg^{2+}	Al^{3+}	Si^{4+}	K^+	Ca^{2+}	Sc^{3+}	Ti^{4+}	Au^+	Hg^{2+}	Tl^{3+}	Pb^{4+}
Electronic configuration	← $[He]2s^22p^6$ ⟶				← $[Ne]3s^23p^6$ ⟶				← $[Xe]4f^{14}5d^{10}$ ⟶			
Total no. of extra-nuclear electrons	← 10 ⟶				← 18 ⟶				← 78 ⟶			
Units of nuclear positive charge	11	12	13	14	19	20	21	22	79	80	81	82
Radius (in pm) (Pauling's value)	95	65	50	41	133	99	81	68	137	110	95	84

Now let us consider the **isosteric anionic species** (see Table 12.4.2). It is evident that with the increase of the anionic charge, the anionic radii change but not so markedly in contrast to the isosteric cationic species. The fact can be rationalised by considering the **two opposing factors.** (a) The increased electron density reduces the nuclear charge/electron ratio, increases the electron-electron repulsion and decreases the effective nuclear charge to be experienced by the outermost electrons. These factors increase the ionic radii. (b) But due to the increased anionic charge, the Coulombic attraction between the cation and anion increases and consequently the **interionic separation shortens.** It leads to a shrinkage in the anionic radii. This fact is also concluded from the Born equation (see Sec. 12.7), *i.e.*

$$R_0 = (r_+ + r_-); \text{ and, } R_0 \propto \left(\frac{1}{Z^+Z^-}\right)^{1/(n-1)} \quad (cf. \text{ Eqn. } 12.3.2.8); \text{ and } r_i = r_1(i)^{-2/(n-1)}, (cf. \text{ Eqn. } 12.3.2.14)$$
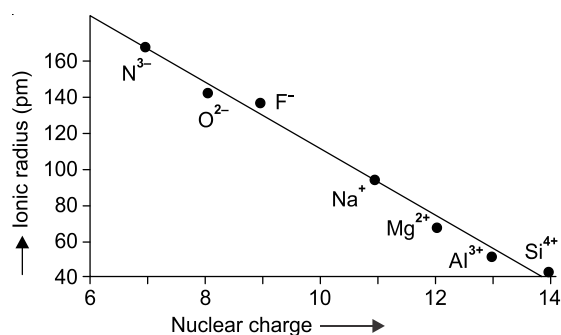
Table 12.4.2. Ionic radii of some **isosteric anions**

Ion :	N^{3-}	O^{2-}	F^-	P^{3-}	S^{2-}	Cl^-	Se^{2-}	Br^-
Electronic configuration:	← $[He]2s^22p^6$ ⟶			← $[Ne]3s^23p^6$ ⟶			← $[Ar]3d^{10}4s^24p^6$ ⟶	
Total no. of extranuclear electrons:	← 10 ⟶			← 18 ⟶			← 36 ⟶	
Units of nuclear positive charge:	7	8	9	15	16	17	34	35
Radius (in pm) (Pauling's value):	170	140	136	212	184	181	198	195

Because of the two opposing factors, the ionic radius does not change so remarkably with the change of charge on the isosteric anions.

Fig. 12.4.1. Variation of ionic radii with the nuclear charge of the ions of electronic configuration of neon.

(iii) *Influence of coordination number, i.e. crystal geometry* : With the increase of coordination number, the interionic separation and consequently the ionic radius increases. It is due to the fact that the more the number of surrounding ions, the less is the **share of the attraction** to be experienced by each of the oppositely charged ions. In addition to this, it can be said that with the increase of coordination number, to avoid the **steric hindrance** among the coordinating or surrounding ions, they tend to keep themselves away from the central ion. For example, if 8 Cl^- ions instead of 6 Cl^- ions are to coordinate the central ion, *e.g.* Na^+, then the Cl^- ions in the 8 coordination system cannot approach towards the Na^+ ion up to the distance as attained by the Cl^- ions in the 6 coordination system. If we want to place

the 8 Cl^- ions at the same distance as in the 6 coordination number, then there will be a severe repulsion among the Cl^- ions due to the steric hindrance. This is why, the interionic separation between the adjacent opposite ions always increases with the increase of the coordination number.

The fact can be quantitatively supported by the Born equation (see Sec. 12.7) which leads to :

$$R_0 = r_+ + r_- = \left(\frac{nB4\pi\varepsilon_0}{AZ^+Z^-e^2} \right)^{1/(n-1)} = \left(\frac{n4\pi\varepsilon_0}{Z^+Z^-e^2} \right)^{1/(n-1)} (B/A)^{1/(n-1)}$$

From the above equation, it is evident that the interionic separation (R_0) depends on B, *i.e.* the type of the crystal. If we consider that an ionic compound AB may be crystallised in both **common salt structure (*i.e.* *NaCl*, 6:6) and cesium chloride structure (*i.e.* *CsCl*, 8:8)**, then the interionic separations (R_0) in AB in the two forms are related as follows :

$$\boxed{R_{0(NaCl)} / R_{0(CsCl)} = [(B_{NaCl}A_{CsCl})/(B_{CsCl}A_{NaCl})]^{1/(n-1)}}$$

where B measures the **short range repulsive force.** Hence to measure B, we can reasonably consider the only nearest neighbours. Thus we get :

$$B_{NaCl}/B_{CsCl} = 6/8$$

The ratio of the Madelung constants is given by,

$$A_{CsCl}/A_{NaCl} = 1.76267/1.74755 \approx 1.0$$

Thus, $$R_{0(NaCl)}/R_{0(CsCl)} = (B_{NaCl}/B_{CsCl})^{1/(n-1)} = (6/8)^{1/(n-1)}.$$

For, $n = 9$ (*i.e.* *Ar* gas configuration), $R_{0(NaCl)}/R_{0(CsCl)} = 0.965$.

Thus if a compound exists in both *NaCl* and *CsCl* structure, **the interionic separation in the *CsCl* crystal will be ~ 3% larger than that in the *NaCl* structure.** Similar calculations may be done for other crystals to illustrate the dependance of ionic radii on the crystal structure. It is found that the interionic separation in the *NaCl* structure is ~ 5% more compared to that in the zinc blende (*ZnS*) structure. Thus we can write,

> **Coordination No :** (*ZnS*, *Zn* - blende, 4:4),   (*NaCl*, 6:6), (*CsCl*, 8:8)
> **R_0 (= $r_+ + r_-$)**   0.95   1.00   1.037
> (relatively)

C.N. :	4	5	6	7	8	12
$r(Na^+)$ (pm) :	112	114	116	125	132	138

Thus it is evident that the absolute difference in the values for different crystals is not significantly large. But, if required, we can use the multiplication factors to compute the ionic radii from one crystal system to another. Here it is important to mention that the Pauling's radii were calculated assuming the 6:6 coordination number as in *NaCl* and *NaF*.

(iv) ***Influence of the radius ratio* :** As the radius ratio (r_+/r_-) tends to the lower limiting value for a particular geometry, the **anion-anion repulsion** increases (see Sec. 12.8) and it will tend to increase the interionic separation and consequently the ionic radii. For the octahedral geometry as in the *NaCl* structure, the limiting radius ratio is ~ 0.41 and the structure can be attained in the range of ratio ~ 0.41 to 0.73. **However, if the radius ratio tends to the lower limiting value, 0.41 then the interionic separation increases.** It is evident from Table 12.4.3.

In computing the Pauling's radii, no such **anion-anion repulsion** was considered. In fact, no such repulsion exists in reality when $r_+/r_- \approx 0.7$ as in *NaF*. Thus for the systems having the radius ratio ~ 0.7, there is no discrepancy between the experimental and calculated value, but

Table 12.4.3. Effect of radius ratio on the interionic separation (in pm) in *NaCl* type (6 : 6) structure

Compound	r_+/r_-	$R_0 = r_+ + r_-$ (calculated from Pauling's radii)	R_0 (experimental)
RbBr	0.76	343	343
KBr	0.68	328	329
NaBr	0.49	290	298

as the ratio tends to the lower limiting value (*e.g.* 0.41 in the octahedral system), the repulsion increases to increase the interionic separation leading to an appreciable discrepancy. **In explaining the relatively lower melting points (see Fig. 12.7.5.1) of *LiF* (r_+/r_- = 0.44) and *NaI* (r_+/r_- = 0.44), the anion-anion repulsion was considered to reduce the cohesive energy.** Fig. 12.7.5.1 thus establishes the fact that in tending towards the lower (r_+/r_-) limiting radius ratio value, the anion-anion repulsion increases.

(v) ***Effect of polarisation* (*i.e. covalency*) :** The ionic radius of a particular ion in a compound is dependent on the degree of polarisation or covalency present in the compound. ***With the increase of covalency, the radius of a cation increases while the radius of an anion decreases.*** The effect of covalency on the radius of H^- is well noted in the alkali metal hydrides (see Table 12.3.4.2). If in attaining the covalency, the cation utilises its new principal quantum number as in the case of alkali and alkaline earth cations, the size of the cation gets remarkably increased. The alkali and alkaline earth cations use the next outer ns orbital to introduce the covalency.

(vi) ***Crystal field effect* :** In terms of crystal field theory (CFT), a transition metal ion in an octahedral geometry shows a lower value of its ionic radius in low spin state compared to its value in high spin state. *In fact, various factors like spin state, geometry and electronic configuration are important to determine the crystal radii of transition metal ions*. Discussion on these aspects has been done in Vol. 4.

In the *octahedral systems*, some representative Shannon's values (in pm) are :

Ions :	Cr^{2+}	Mn^{2+}	Fe^{2+}	Co^{2+}	Fe^{3+}	Co^{3+}
r (low spin) :	87	81	75	79	69	68
r (high spin) :	94	97	92	89	78	75

12.5 ENERGETICS OF IONIC BOND FORMATION : BORN-HABER CYCLE

12.5.1 Born-Haber Cycle for Ionic Bond Formation

In predicting the possibility of an ionic bond formation in a particular compound, it is more important to consider the energetics of the process of formation rather than the concept of attaining the stable electronic configuration of the constituent ions in the compound under consideration. If the process is exothermic* (*i.e.* $\Delta H < 0$), the compound is stable, but if the process is endothermic (*i.e.* $\Delta H > 0$) the compound is unstable. The enthalpy change (*i.e.* ΔH) of the process can be computed from the Born-Haber cycle which is based on the basic principle (Hess's law) of thermochemistry. ΔH being a state function does not depend on the path through which the process is carried out but on the initial and final state.

---

* More correctly, to predict the stability we should consider ΔG (= $\Delta H - T\Delta S$) rather than ΔH alone. **But in the formation of an ionic lattice starting from a solid metallic crystal, ΔS is not very much significant.** Here, at an ordinary condition, consideration of ΔH predicts almost the correct result.

ΔH of the process leading to an ionic crystal may be obtained experimentally by the direct combination of the constituent elements. It can also be computed by using the Born-Haber cycle which involves the following steps :

(i) Vaporisation of the involved reactant elements.

(ii) Formation of the required ions from the isolated gaseous atoms.

(iii) Combination of the gaseous ions to produce the solid product.

To illustrate the principle of Born-Haber cycle, let us consider the formation of the simple ionic compound M^+X^- (*e.g. NaCl*) in computing the **standard molar enthalpy of formation (ΔH_f)** which is defined as the change of enthalpy in the formation of one mole of the ionic compound M^+X^- from its constituent elements in their most stable physical states at 298 K and 1 atm pressure.

Formation of M^+X^- can be considered to take place in two paths (assuming M and X_2 to exist in solid and gaseous state respectively at ordinary condition) as shown in the Scheme 12.5.1.1.
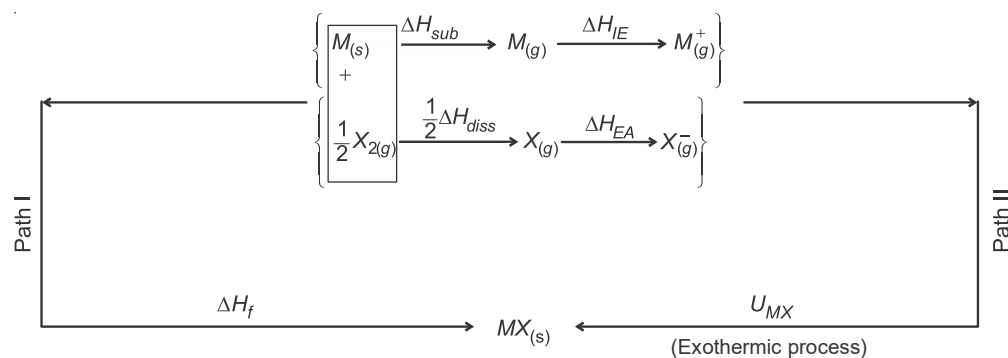
Scheme 12.5.1.1. Possible paths leading to the formation of M^+X^- crystal.

(Note: Formation of $MX_{(s)}$ (solid ionic lattice) from the gaseous ions may be considered to pass through the formation of *gaseous ion-pair*, $M^+X^-_{(g)}$.
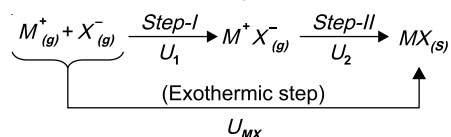
For the sake of simplicity, the gaseous ion-pair formation step has been ignored in Scheme 12.5.1.1. The energy change in the overall process (*i.e.* combination of Step I and Step II) has been described here as the **lattice energy** (U_{MX}). Thus, $U_{MX} = U_1$ (for the gaseous ion-pair formation) + U_2 (for lattice formation). For the formation of sodium chloride (*NaCl*), U_1 and U_2 have been theoretically calculated ($U_1 \approx -440$ kJ mol^{-1} and $U_2 \approx \sim 330$ kJ mol^{-1}).

Path II consists of the following steps :

(i) **First step :** It involves the sublimation of solid M into its vapour. It requires the *sublimation energy*, ΔH_{sub}.

(ii) **Second step :** It involves the ionisation of the isolated gaseous atoms of M. It requires the *ionisation energy* (*i.e.* first *IE*), ΔH_{IE}.

(iii) **Third step :** It involves the *bond dissociation* of the halogen gas X_2 (say Cl_2) to form the gaseous atoms. As the process requires half mole of X_2 to form one mole of MX, the requirement of energy is $\frac{1}{2}\Delta H_{diss}$.

(iv) **Fourth step :** It involves the gaining of an electron by the isolated gaseous atom (X) to form X^-. It measures the **electron affinity**, ΔH_{EA}.

(v) ***Final step* :** It involves the combination of the oppositely charged isolated gaseous ions (in the gaseous phase, they may exist as the ion pairs, but here we are ignoring this aspect for the sake of simplicity) to form a solid crystal in which the omnidirectional electrostatic force works throughout the crystal. It leads to the **release of lattice energy,** U_{MX} which may be considered as the ***lattice enthalpy*** (ΔH_L). Thus, we get the following relation with *appropriate signs of the energy terms* (according to the convention of thermodynamics).

$$\Delta H_f = \Delta H_{sub} + \Delta H_{IE} + \frac{1}{2}\Delta H_{diss} + \Delta H_{EA} + U_{MX} \qquad \dots(12.5.1.1)$$

From the standard convention of thermodynamics, when the energy is released (*i.e.* exothermic) it is associated with a **negative sign (–ve)** while for the energy requiring (*i.e.* endothermic) process, the energy term is associated with a **positive sign (+ve)**. In forming the lattice from the isolated gaseous ions, the energy measured by lattice energy (U_{MX}) is released. Generally the energy term (ΔH_{EA}) measuring the electron affinity is exothermic. In the case of *NaCl*, by using the calculated value of lattice energy and other energy terms experimentally determined, let us calculate the enthalpy of formation (ΔH_f). $\Delta H_{sub} = 108.8$ kJ mol^{-1}, $\Delta H_{IE} = 493.8$ kJ mol^{-1}, $\frac{1}{2}(\Delta H_{diss}) = 121.3$ kJ mol^{-1}, $\Delta H_{EA} = -348.5$ kJ mol^{-1}, $U_{NaCl} = -757.3$ kJ mol^{-1}. By using these energy values in Eqn. 12.5.1.1, we get, $\Delta H_f = -381.9$ kJ mol^{-1}. This calculated value can be compared with the experimental one, -411 kJ mol^{-1}. The calculation from the Born-Haber cycle shows that the formation of $Na^+Cl^-_{(s)}$ is exothermic and it occurs so in reality.

Note 1 (Hess's law and Born–Haber thermodynamic cycle dealing with the standard enthalpy change): Hess's law states that the **standard enthalpy change** (denoted by ΔH^0) of a process is the sum of the standard enthalpy changes of the individual steps of the overall process. Thus in Born–Haber cycle, we should strictly use the **standard enthalpy values of all steps**. **Standard enthalpy change denotes the change of enthalpy for a process/step in which the initial and final substances are in their standard states**.

The **standard state of a substance** at a specified temperature is its pure form at 1 bar pressure. However, very often, the standard pressure is taken as 1 atm (= 101.325 kPa) instead of 1 bar (= 100 kPa). The standard enthalpy change may be at any temperature depending on the condition at 1 bar pressure (*e.g.* H_2O (*s*) $\rightarrow H_2O$ (*l*), ΔH^0 (273 K) = +6.01 kJ mol^{-1}; H_2O (*l*) $\rightarrow H_2O$ (*g*), ΔH^0 (373 K) = +40.65 kJ mol^{-1}). However, conventionally, 298 K (*i.e.* 25°C) is chosen (if not mentioned other temperature) for reporting the thermodynamic data.

Thus in Born–Haber cycle, strictly, the **standard enthalpy values (denoted by ΔH^0)** are to be used as illustrated for the formation of $CaBr_2$(s) in Scheme 12.5.1.2. However, for the **sake of simplicity, the superscript (0) has been omitted very often in this book to construct the Born–Haber cycle**.

Note 2 (Relation between the enthalpy values and the commonly used energy values in different steps/processes): It has been mentioned that enthalpy is a **thermodynamic state function** and its change is path independent. Thus in Born–Haber cycle, **enthalpy values are to be strictly used** for all steps. In Scheme 12.5.1.1, ionisation energy (instead of ionisation enthalpy), electron affinity (instead of the corresponding enthalpy value), have been used as their enthalpy values for the sake of simplicity. Now let us examine **whether the approximation is justified or not**. It is illustrated for the ionisation process. **Ionisation enthalpy (ΔH_{IE}) equals the so called ionisation energy (IE) at absolute zero** (T = 0 K). For the following ionisation process.

$$M_{(g)} \to M^+{}_{(g)} + e_{(g)}, \qquad \Delta H_{IE(T)} = \text{Ionisation enthalpy at T K}$$

$$= \Delta H_{IE(0)} + \int_0^T \Delta C_P dT = IE + \int_0^T \Delta n \bar{C}_P dT$$

$$= IE + \frac{5}{2} RT \text{ (see Sec. 8.12)}$$

$\bar{C}_P = \frac{5}{2} R$ (for a monoatomic gaseous species having the translational motions only).

$\Delta H_{IE(298)}$ is called the **standard enthalpy of ionisation** which differs from *IE* by $\frac{5}{2} R \times 298$ (≈ 6.2 kJ mol^{-1}), a **negligible quantity compared to the *IE* value.**

Similarly, **the electron affinity value, lattice energy value, bond dissociation energy value**, etc. **give their corresponding enthalpy values only** at 0 K. In all such cases, the **temperature correction factor is quite a negligible quantity**. This is why, these energy values are generally used as their enthalpy values in thermodynamics calculations as illustrated in Scheme 12.5.1.1. However, Scheme 12.5.1.2 illustrates the **use of true enthalpy values** (without the said approximation) but the result does not differ significantly from the result obtained by ignoring the temperature correction factor.

Note 3 (Definition of lattice enthalpy and energy): Standard lattice enthalpy ($\Delta H_{L(298)}$) is given by the standard molar enthalpy change for the **conversion of the solid ionic crystal into the constituent ions in the gaseous state.**

$$MX_{(s)} \to M^+_{(g)} + X^-_{(g)}, \Delta H_L = +\text{ve (Endothermic process)}$$
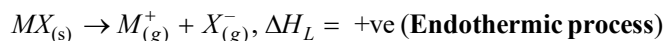
ΔH_L **becomes lattice energy (U_{MX}) at T = 0 K** as in the case of ionisation process. It has been already mentioned that for the sake of simplicity, U_{MX} may be taken as the ΔH_L.

Lattice enthalpy (ΔH_L) or lattice energy (U) may be also defined with respect to the following process leading to the **formation of solid ionic crystal from the constituent gaseous ions** (as illustrated in Scheme 12.5.1.1 and in Sec. 12.7.1).

$$M^+_{(g)} + X^-_{(g)} \to MX_{(s)}, \Delta H_L = -\text{ve (Exothermic process)}$$
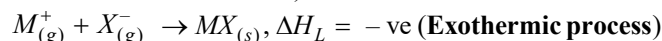
Both the concepts with proper signs are available in the text books. However, some authors strictly refer to the **endothermic process** (*i.e.* positive energy term) corresponding to the break-up of lattice. The positive sign (+) to express the lattice enthalpy or lattice energy is omitted from the numerical value.
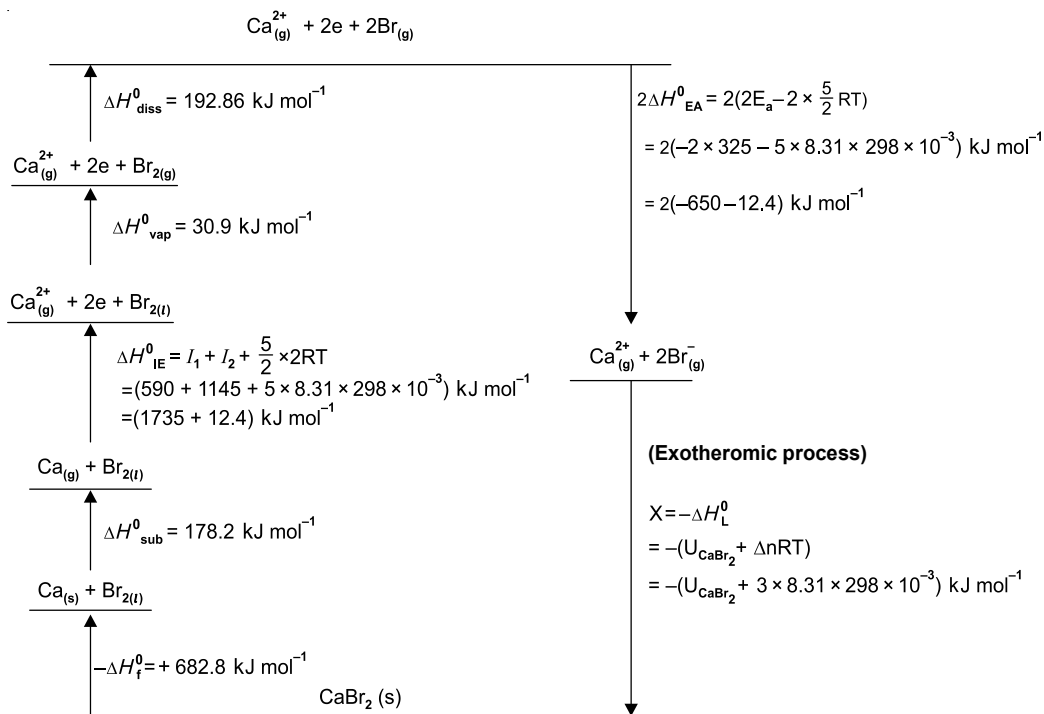
Note 4 (Thermodynamic feasibility determined by Gibbs free energy change not alone by the enthalpy parameter): Born–Haber cycle allows to compute the enthalpy change of a particular process but to determine the **thermodynamic feasibility** of a process, the Gibbs free energy change (more correctly, the standard free energy change, $\Delta G^0 = \Delta H^0 - T\Delta S^0$) is to be considered (*i.e.* $\Delta G^0 = $ –ve for a thermodynamically allowed process). Hence to determine the thermodynamic feasibility, both the enthalpy factor and entropy factor are to be considered. However, in the case **formation of solid ionic crystals** from their constituents (as illustrated in Schemes 12.5.1.1, 2), the contribution of **entropy factor (specially at low temperature)** may be ignored to determine the thermodynamic feasibility of the process. Strictly, this approximation is valid at $T = 0$ K (where $T\Delta S^0 = 0$). In fact, in the formation of solid ionic crystal, ΔS^0 becomes slightly negative due to the formation of a highly ordered ionic crystal. Thus, ΔG^0 **becomes negative only when** ΔH^0 **becomes highly negative in such cases.**

● **Thermodynamic criterion of spontaneity for a reaction and relationship between ΔG and ΔG^0:** ΔG^0 denotes the standard free energy (**standard state** refers to 1.0 mol dm^{-3} concentration for each reactant and product). For a reaction to go on spontaneously, ΔG (*i.e.* change in Gibbs free energy) is to be negative. ΔG and ΔG^0 for the following reaction are related as follows:

$$A + B \rightleftharpoons C + D, \Delta G = \Delta G^0 + RT \ln \frac{[C][D]}{[A][B]}$$

Thus ΔG depends on the concentrations of the reactants and products and this contribution is determined by the second term of the above equation. **The criterion of spontaneity for a reaction is ΔG = –ve (irrespective of the sign of ΔG^0).** The standard energy change (ΔG^0) and the thermodynamic equilibrium constant K_{eq}^0 (**a dimensionless quantity**) under the standard conditions are related as follows:

$$\Delta G^0 = -RT \ln K_{eq}^0, \Delta G^0 = -\text{ve for } \ln K_{eq}^0 > 1$$

$Ca_{(g)}^{2+} + 2e + 2Br_{(g)}$

$\Delta H^0_{diss} = 192.86 \text{ kJ mol}^{-1}$

$2\Delta H^0_{EA} = 2(2E_a - 2 \times \frac{5}{2} RT)$

$= 2(-2 \times 325 - 5 \times 8.31 \times 298 \times 10^{-3}) \text{ kJ mol}^{-1}$

$= 2(-650 - 12.4) \text{ kJ mol}^{-1}$

$Ca_{(g)}^{2+} + 2e + Br_{2(g)}$

$\Delta H^0_{vap} = 30.9 \text{ kJ mol}^{-1}$

$Ca_{(g)}^{2+} + 2e + Br_{2(l)}$

$\Delta H^0_{IE} = I_1 + I_2 + \frac{5}{2} \times 2RT$
$= (590 + 1145 + 5 \times 8.31 \times 298 \times 10^{-3}) \text{ kJ mol}^{-1}$
$= (1735 + 12.4) \text{ kJ mol}^{-1}$

$Ca_{(g)}^{2+} + 2Br_{(g)}^-$

(Exotheromic process)

$Ca_{(g)} + Br_{2(l)}$

$\Delta H^0_{sub} = 178.2 \text{ kJ mol}^{-1}$

$X = -\Delta H^0_L$
$= -(U_{CaBr_2} + \Delta nRT)$
$= -(U_{CaBr_2} + 3 \times 8.31 \times 298 \times 10^{-3}) \text{ kJ mol}^{-1}$

$Ca_{(s)} + Br_{2(l)}$

$-\Delta H^0_f = +682.8 \text{ kJ mol}^{-1}$

$CaBr_2 \text{ (s)}$

Scheme 12.5.1.2. Born–Haber cycle for the formation of $CaBr_2$.

• **Illustration of strict thermodynamic convention: Calculation of lattice enthalpy (ΔH_L) or lattice energy (U) of $CaBr_2$ from the Born–Haber cycle.**

The corresponding Born–Haber cycle for the formation of $CaBr_2$(s) is illustrated in Scheme 12.5.1.2 where the **standard enthalpy values** ($\Delta H°$) have been used.

• **Standard state** (denoted by superscript 0) conventionally refers to 298 K temperature.

ΔH^0_f = standard enthalpy of formation of $CaBr_2 = -682.8 \text{ kJ mol}^{-1}$

ΔH^0_{sub} = standard enthalpy of sublimation of $Ca = 178.2 \text{ kJ mol}^{-1}$

ΔH^0_{vap} = standard enthalpy change of vaporisation of $Br_{2(l)} = 30.9 \text{ kJ mol}^{-1}$

ΔH^0_{diss} = standard enthalpy of bond dissociation of $Br_{2(g)}$

$\approx$ standard bond dissociation energy of $Br_{2(g)}$ see Sec. 10.1.2)

$= 192.86 \text{ kJ mol}^{-1}$

(ΔH^0_{diss} – standard bond dissociation energy $\approx 2.5 \text{ kJ mol}^{-1}$, see Sec. 10.1.2).

ΔH^0_{1E} = standard enthalpy change during the ionisation of $Ca_{(g)}$ (i.e. $Ca_{(g)} \rightarrow Ca_{(g)}^{2+} + 2e_{(g)}^-$)

$= I_1 + I_2 + \frac{5}{2}\Delta nRT$

$= (590 + 1145 + 5 \times 8.31 \times 298 \times 10^{-3}) \text{ kJ mol}^{-1}$

$= (1735 + 12.4) \text{ kJ mol}^{-1}$